BEAM INDUCED POWER LOSS ESTIMATION OF A MOVABLE SYNCHROTRON LIGHT EXTRACTION MIRROR FOR THE LHC

W. Andreazza, E. Bravin, F. Guillot-Vignot, M. Wendt*, CERN, Geneva, Switzerland

Abstract

Beam instruments based on synchrotron light are an important part of the beam monitoring diagnostics suite in the Large Hadron Collider (LHC) at CERN. In frame of the high luminosity upgrade (HL-LHC) additional synchrotron light diagnostics are demanded, too many to be covered by the present Beam Synchrotron-light Radiation Telescope (BSRT), which utilizes the light extraction mirror in a fixed position. Therefore, an additional synchrotron light diagnostics setup is under development, now with a movable mirror to extract the synchrotron light emitted solely by a superconducting LHC dipole magnet. With higher bunch intensities anticipated in the HL-LHC, the beam induced power losses, and therefore local heat dissipation, play a critical role in the design of the extraction mirror. This paper summarizes the estimation of the bunched-beam induced power losses based on numerical simulations and RF measurements on a prototype light extraction mirror.
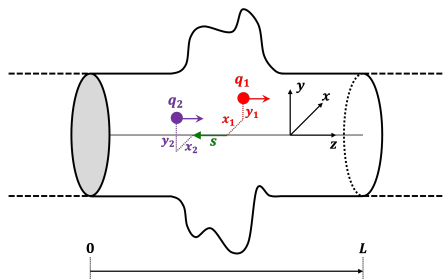
INTRODUCTION

Figure 1: Definition of wakefields.

Any component or device, e.g. a beam manipulation device, a beam pickup or any other beam vacuum component that presents a discontinuity or change of geometry of the beam pipe of an accelerator alters the electromagnetic field of a leading source point charge q_1, and causes *wakefields* which acts on a trailing test point charge q_2, see also Fig. 1. The integration of the *Lorenz* force

$$\mathbf{F} = \frac{d\mathbf{p}}{dt} = q_2 \left(\mathbf{E} + c\mathbf{e_z} \times \mathbf{B} \right) \quad (1)$$

over the relevant length L of the accelerator component leads to the *wake function* [1]

$$\mathbf{w}(x_1, y_1, z_1, s) = \frac{1}{q_1} \int_0^L dz \left[\mathbf{E}(x_2, y_2, z, t) + c\mathbf{e_z} \times \mathbf{B}(x_2, y_2, z, t) \right]_{t=(s+z)/c} \quad (2)$$

---

* manfred.wendt@cern.ch

The *Fourier* transformation of the wake function Eq. (2) is called *beam-coupling impedance*

$$Z_\parallel(x_1, y_1, x_2, y_2, \omega) =$$
$$-\frac{1}{c} \int_{-\infty}^{+\infty} ds \, w_\parallel(x_1, y_1, x_2, y_2, s) e^{-j\omega s/c} \quad (3)$$

Eq. (3) is the definition for the longitudinal coupling impedance, because it is the real part of the longitudinal component $\Re[Z_\parallel(\omega)]$ that causes an energy loss, thus a beam induced power loss, and contributes to the so-called *RF heating* of an accelerator component.

The light extraction mirror of the Beam Synchrotron-light Radiation Telescope (BSRT) was a source of RF heating issues during Run 1 of the Large Hadron Collider (LHC) at CERN [2]. A successful overhaul of the BSRT light extraction mirror solved the RF heating problem, with no issue observed during LHC Run 2. For the high luminosity upgrade of the LHC (HL-LHC) the beam intensity will be doubled [3], and additional measurements based on synchrotron light are foreseen. Therefore, an additional synchrotron light monitor system, the BSRTM is under development, Fig. 2 shows a schematic view as it was used as geometric input for the numerical analysis. As of the new design, utilizing a movable mirror, and as of the anticipated higher beam intensity in the LHC, a prototype of the BRSTM light extraction mirror was build and installed during the long shutdown 2 of the LHC in 2021. This prototype tank is equipped with PT100 temperature sensors to monitor RF heating effects during LHC Run 3, which started in Spring of year 2022.

Before installation, the BSRTM prototype light extraction tank was analyzed applying a stretched-wire RF measurement method to estimate its beam-coupling impedance. This report summarizes the measurement results, along with a numerical analysis and the calculation of the related RF power losses based on the expected HL-LHC beam parameters.
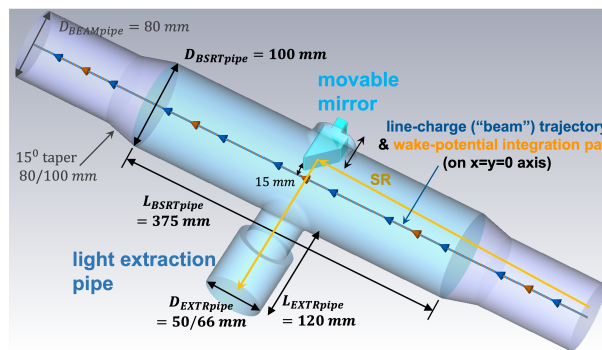

Figure 2: The LHC BSRTM synchrotron-light extraction mirror prototype.

BSRTM IMPEDANCE ANALYSIS

The analysis of the beam-coupling impedance $Z_\parallel$ of the BSRTM synchrotron-light extraction system covered the "blue" elements indicated in Fig. 2, i.e., the 100 mm aperture BSRTM tank pipe, the movable mirror and the light extraction pipe, but not the 80/100 mm taper sections and the attached 80 mm beam pipe stubs ("gray" in Fig. 2). From this configuration we can expect *trapped* resonant modes related to the cut-off frequency of the lowest TE mode of a waveguide with circular cross-section:

$$f_{TE\nu s} = \frac{j'_{\nu s}}{2\pi r \sqrt{\epsilon \mu}} \Rightarrow f_{TE11} \simeq \frac{0.293 c}{r} \qquad (4)$$

with r being the radius of the beam pipe or light extraction pipe, $j'_{\nu s} = j'_{11} \simeq 1.8412$ being the 1st root of the derivative of the *Bessel* function $J'_s = J'_1$ and with the fact dielectric or magnetic materials are absent ($\epsilon_r = \mu_r = 1$).

Numerical Analysis

The numerical analysis was based on the time domain wakefield solver, which is part of the commercial *CST Studio Suite* finite element electromagnetic software. Figure 2 shows both, the bunched beam and the wakefield integration paths are on the z-axis ($x = y = 0$). The simulation setup uses a *Gaussian* line-charge $i(s) = en \exp[s^2/(2\sigma^2 c^2)]/(\sigma \sqrt{2\pi})$ with $\sigma = 37.475$ mm and $n = 1 \times 10^{11}$ particles as stimulus function to evaluate the *wake potential* $\mathbf{W}(s)$ of the structure. The beamcoupling impedance $Z_\parallel(\omega)$ is calculated by a *Fourier* transformation of the wake potential $W_\parallel(s)$, and de-convoluting the *Gaussian* stimulus distribution, here taking frequencies up to 2.73 GHz into account ($\equiv -20$ dB of the *Gaussian* bunch spectrum). For all simulations a wake length of 500 m $\equiv 1.67\,\mu$s was used, the discretization used approximately 2.4×10^6 mesh-cells.
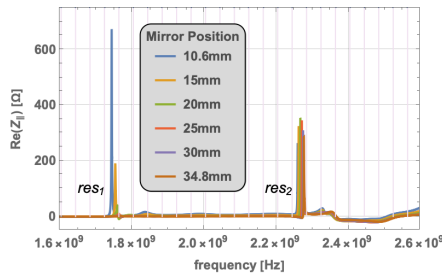

Figure 3: Result of the numerical analysis of $\Re[Z_\parallel(\omega)]$.

Figure 3 shows the results of the numerical analysis for different positions of the light extraction mirror – the distance between mirror edge and beam – clearly indicating two resonances:

- Resonance res_1 at $f_1 \approx 1.75$ GHz is related to f_{TE11} of the beam pipe with $r = D_{BSRTpipe}/2 = 50$ mm.

- Resonance res_2 at $f_2 \approx 2.27$ GHz is related to f_{TE11} of the light extraction pipe.

A detailed field analysis verified both resonances have TE11 mode patterns. and are trapped near the mirror and at the entrance of the light extraction pipe, respectively. The peak value of the beam-coupling impedance of res_1 depends on the mirror position, and this resonance basically vanishes if the mirror position is $\gtrsim 25$ mm. The peak value $\Re[Z_\parallel(f_2)] \approx 300\,\Omega$ is almost independent from the mirror position, in both cases the resonance frequencies shift slightly with the mirror position. For reference, the vertical lines in Fig. 3 indicate the location of the main beam harmonics at multiples of 40.077 MHz.
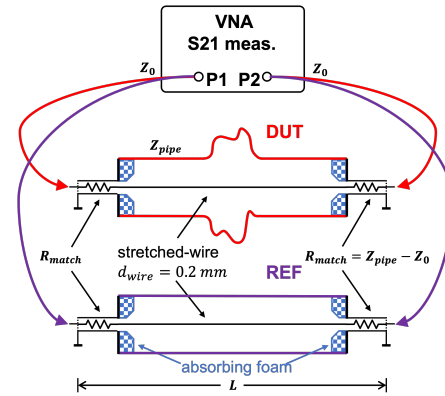
Stretched-Wire RF Measurements

Figure 4: Stretched-wire impedance measurement.

The longitudinal beam-coupling impedance of a *device under test (DUT)* – here the BSRTM light extraction mirror tank – was evaluated through a RF measurement of the $S21$ transmission coefficient of the 2-port scattering (S) parameter matrix, utilizing a vector network analyzer (VNA) [4].

$$Z_\parallel = -Z_{\text{pipe}} \ln(S21) \left[1 + j \frac{\ln(S21)}{2\theta} \right] \qquad (5)$$

with:

$$Z_{\text{pipe}} = \frac{\eta_0}{2\pi \sqrt{\epsilon_r}} \ln \frac{D}{d} \simeq 60 \ln \frac{D_{\text{pipe}}}{d_{\text{wire}}} \approx 373\,\Omega, \quad \theta = 2\pi \frac{L}{\lambda}$$

As illustrated in Fig. 4 it requires two separate $S21$ measurements, one performed on the actual DUT and another one on an unperturbed (straight) reference-line of same physical length L and characteristic impedance Z_{pipe} to evaluate $S21$ as ratio

$$S21 = \frac{S21_{DUT}}{S21_{REF}} \qquad (6)$$

here performed over a frequency range of 4 MHz ... 4 GHz. A low-inductance resistor $R_{match} = Z_{pipe} - Z_0 \approx 330\,\Omega$ is used to match the $Z_0 = 50\,\Omega$ reference transmission-line impedance of the measurement setup to that of the beam pipe $Z_{pipe} \approx 373\,\Omega$. While this lumped element impedance matching works fine for low frequencies $\lesssim 1$ GHz, absorbing foam was applied at the coaxial discontinuities which reduced reflection effects successfully to frequencies up to approximately 2.5 GHz.
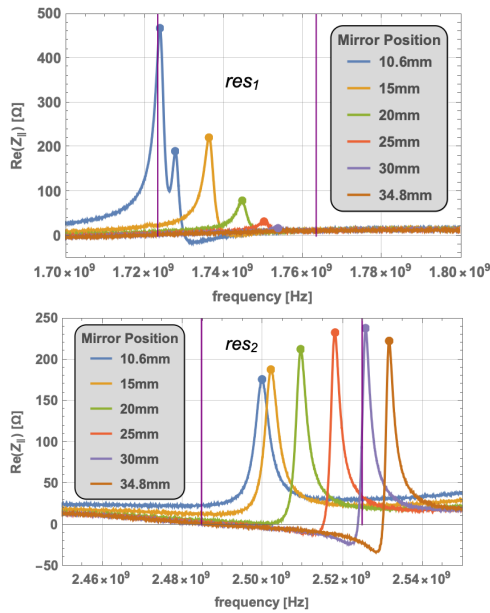
Figure 5: Stretched-wire impedance measurements.

Figure 6: Measured LHC beam spectrum and analytical single bunch approximation.

The stretched-wire RF measurement returned a result similar to that of the numerical analysis, Fig. 5 shows $\Re[Z_\parallel(\omega)]$ for different mirror positions separately for *resonance 1* (upper plot) and for *resonance 2* (lower plot). In the measurement the higher frequency resonance 2 appears at 2.52 GHz, compared to 2.27 GHz for the numerical simulation, which is likely due to some simplifications in the numerical analysis, e.g., details on the bellow were not taken into account, also a simple electric boundary was used instead of modeling all the details of the vacuum window.

RF POWER LOSSES

The RF power losses are calculated based on *Ohm's* law

$$P_{loss} = I_{beam}^2 Z_{loss} = 2I_{beam}^2 \sum_{p=0}^{\infty} |\Lambda(p\omega_0)|^2 \Re[Z_\parallel(p\omega_0)]$$

$$= 2I_{beam}^2 \sum_{i=1}^{n} |\Lambda(\omega_i)|^2 \Re[Z_\parallel(\omega_i)] \quad (7)$$

with $I_{beam} = I_{bunch}N_{bunch}$, were N_{bunch} is the number of bunches of equal intensity and $I_{bunch} = nef_0$. In our case with only two narrowband resonances, $i = 1, 2$, we can simplify the general sum over a wide range of $p\omega_0$ revolution harmonics to just the two resonance frequencies ω_1, ω_2. Furthermore, we replace the complicated LHC beam spectrum by a normalized single bunch spectrum $\Lambda(\omega)$ based on an analytical *Tsallis* q-*Gaussian* function for the longitudinal bunch distribution

$$i_{bunch}(t) = ne\sqrt{\frac{1-q}{2\pi}} \frac{\left[1 + \frac{(q-1)t^2}{2\beta^2}\right]^{\frac{1}{1-q}} \Gamma\left(\frac{3}{2} - \frac{1}{1-q}\right)}{\beta \, \Gamma\left(1 + \frac{1}{1-q}\right)} \quad (8)$$

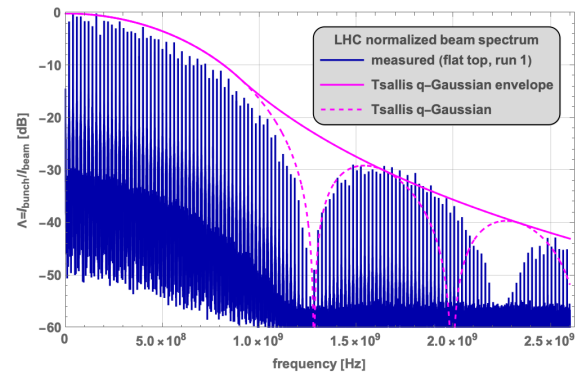with $\beta = \sqrt{(1-q)/2}\, t_{bunch}/2$. The *Fourier* transformation

of Eq. (8), normalized to I_{beam}, gives the single bunch beam spectrum $\Lambda(f)$, which fits reasonable well with the measured LHC beam spectrum for $t_{bunch} = 1.5$ ns and $q = 0.55$, see the dashed line in Fig. 6 in a logarithmic representation $20\log_{10}[\Lambda(f)]$.
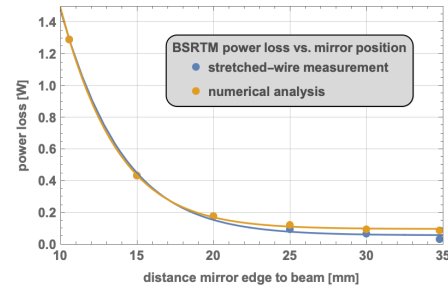

Figure 7: Beam-induce power losses of the BSRTM.

For the calculation of the power losses Eq. (7) however, we use the *envelope* of $\Lambda(\omega_i)$, as illustrated in Fig. 6 to stay on the "safe" side. Figure 7 illustrates the beam induced power losses for different mirror positions for both, the RF measurements and the numerical analysis, using the expected maximum HL-LHC beam intensity $I_{beam} = 1.14$ A. A numerical analysis including the 80/100 mm taper sections, as illustrated in gray in Fig. 2 leads to additional resonances, and also enhances *resonance 1*, therefore in the final installation configuration the tapers should be located more far away from the mirror.

CONCLUSIONS

Stretched-wire RF measurements and numerical analysis for the longitudinal beam-coupling impedance of the new BSRTM synchrotron light extraction mirror, to be deployed for the HL-LHC, show a good agreement which results in beam-induce power losses below 1.5 W under all operational conditions.

REFERENCES

[1] M. Dohlus and R. Wanzenberg, "An Introduction to Wake Fields and Impedances', *Proceedings of the CERN Accelerator*

School CAS: Intensity Limitations in Particle Beams, Geneva, Switzerland, 2-11 November 2015; CERN Yellow Reports, Vol. 3/2017, CERN-2017-006-SP.

[2] W. Andreazza, *et al.*, "Electromagnetic Coupling between High Intensity LHC Beams and the Synchrotron Radiation Monitor Light Extraction System", in *Proc. 4th Int. Particle Accelerator Conf. (IPAC'13)*, Shanghai, China, May 2013, paper TUPFI063, pp. 1493–1495.

[3] "High-Luminosity Large Hadron Collider (HL-LHC) Technical Design Report", CERN-2020-010, ISBN 987-92-9083-587-5, CERN, Geneva, Switzerland.

[4] H. Damerau, *et al.*, "Suggested RF Measurements", CERN CAS Advanced Course, CAS 2019, RF-Lab, pp. 38–40, Slangerup, Denmark.